Bull. Soc. R. Sci. Liège, 2024, **93**(3), 103–119 *Peer-reviewed conference paper*
doi:10.25518/0037-9565.12289

Runaway O and Be Stars Found Using *Gaia* DR3, New Stellar Bow Shocks and Search for Binaries

Mar CARRETERO-CASTRILLO[1], Marc RIBÓ[1,#,*], Josep M. PAREDES[1] and Paula BENAGLIA[2]

[1] Departament de Física Quàntica i Astrofísica, Institut de Ciències del Cosmos (ICCUB), Universitat de Barcelona (IEEC-UB)
[2] Instituto Argentino de Radioastronomía (CONICET–CICPBA–UNLP)
[#] Serra Húnter Fellow
[*] Corresponding author: mribo@fqa.ub.edu

Paper presented at the 41st Liège International Astrophysical Colloquium on "The eventful life of massive star multiples," University of Liège (Belgium), 15–19 July 2024.

Abstract

A relevant fraction of massive stars are runaways, moving with a significant peculiar velocity with respect to their environment. Kicks from supernova explosions or the dynamical ejection of stars from clusters can account for the runaway genesis. We have used *Gaia* DR3 data to study the velocity distribution of massive O and Be stars from the GOSC and BeSS catalogs and identify runaway stars using a 2D-velocity method. We have discovered 42 new runaways from GOSC and 47 from BeSS, among a total of 106 and 69 runaways found within these catalogs, respectively. These numbers imply a percentage of runaways of $\sim 25\%$ for O-type stars $\sim 5\%$ for Be-type stars. The higher percentages and higher velocities found for O-type compared to Be-type runaways suggest that the dynamical ejection scenario is more likely than the supernova explosion scenario. We have also performed multi-wavelength studies of our runaways. We have used WISE infrared images to discover 13 new stellar bow shocks around the runaway stars. We have also conducted VLA radio observations of some of these bow shocks. Finally, our runaway stars include six X-ray binaries and one gamma-ray binary, implying that new such systems could be found by conducting detailed multi-wavelength studies. In this work we report on this ongoing project to find new runaway stars, study their interaction with the ISM and search for high-energy binary systems.

Keywords: massive stars, runaway stars, stellar bow shocks

1. Introduction

Massive early-type OB stars are the brightest stars in the Milky Way and play a crucial role in studying the dynamics of young stellar populations, metallicity enrichment, and feedback processes in the interstellar medium (ISM) due to gamma-ray bursts and supernovae (Vanbeveren et al., 1998; Woosley and Bloom, 2006; Marchant and Bodensteiner, 2024). O-type stars

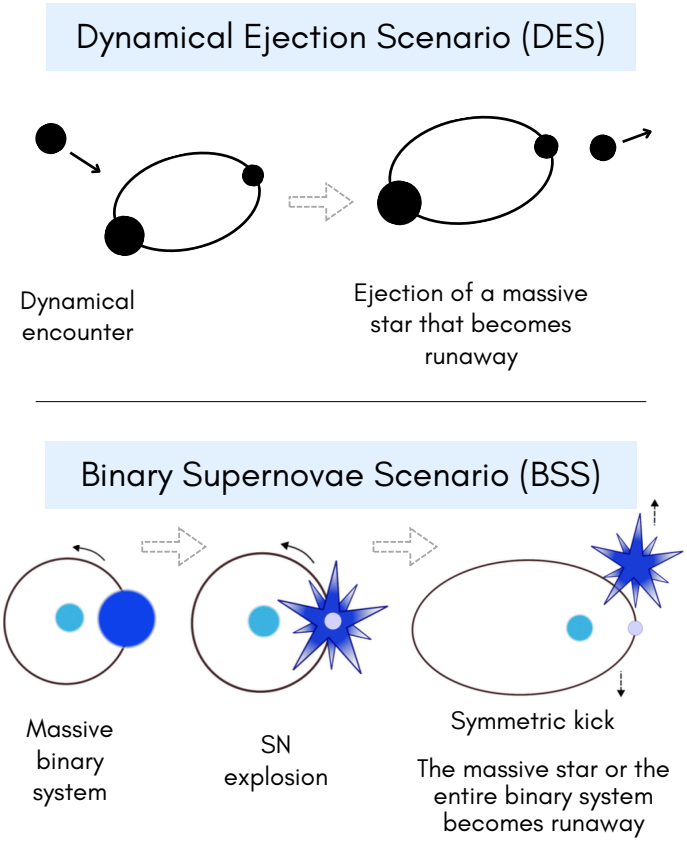

Figure 1: Different scenarios for the production of massive runaway stars.

have short lifespans ($<$ 10 million years) and powerful stellar winds, while B-type stars can live up to 100 million years. Be stars, a subclass of B stars, exhibit Balmer emission lines and infrared excess due to circumstellar decretion disks (Slettebak, 1988; Rivinius et al., 2013).

OB stars are predominantly found in binary systems, with at least 70% forming interacting binaries (Chini et al., 2012; Sana et al., 2012). These systems can evolve into high-mass X-ray binaries (HMXBs), gamma-ray binaries (see Dubus 2013), and other exotic systems, enabling the study of non-thermal processes. A significant fraction of O and B stars are classified as runaway stars, exhibiting high peculiar velocities (Blaauw, 1961; Stone, 1979; Boubert and Evans, 2018). Their formation is explained by two scenarios: the dynamical ejection scenario (DES; Poveda et al., 1967) and the binary supernova scenario (BSS; Blaauw, 1961). A two-step ejection process combining both scenarios might also apply in some cases (Pflamm-Altenburg and Kroupa, 2010). We show in Fig. 1 a schematic representation of the DES and BSS scenarios. We emphasize here that the BSS, in particular, can give rise to the formation of runaway binary systems harboring compact objects, which could eventually be HMXBs or gamma-ray binaries. It is worth noting that some works favor the dominance of the DES scenario (Dorigo Jones et al., 2020) while others favor the dominance of the BSS one (Sana et al., 2022).

Extensive research has been conducted to identify massive runaway stars. This includes the use of different data sets: O stars, OB stars, Be stars, young stars with different spectral types,

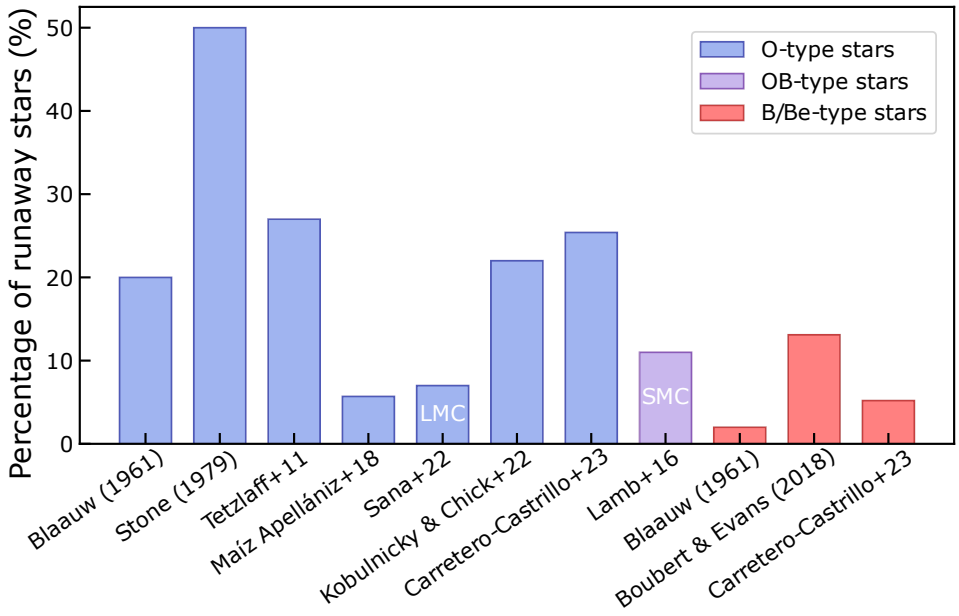

Figure 2: Histogram of the percentage of runaway stars in the Milky Way, and in the LMC and SMC where indicated.

objects in the Milky Way, in the Large Magellanic Cloud (LMC) or in the Small Magellanic Cloud (SMC). In addition, different methods have been used: radial velocities alone, 2D proper motions, 2D velocities, 3D velocities, using thresholds or not, etc. This has an influence in the obtained results. We show the percentage of runaway stars in the Milky Way, LMC and SMC published in several previous works in Fig. 2 and provide more information in Table 1. As it can be seen, apart from very early studies, the percentage of O-type runaway stars is around 20–30%, while that of B and Be stars is around 5–10%. Given the somewhat large dispersions and the publication of *Gaia* data with excellent proper motions and parallaxes, it looks natural to conduct a more refined and comprehensive study.

On the other hand, a stellar bow shock forms when a runaway star with a strong stellar wind travels through the ISM, causing ISM matter to accumulate. If the star's velocity exceeds the local sound speed (typically several kilometers per second), supersonic shocks occur around a boundary that separates the stellar wind from the surrounding medium. These structures, consisting of warm dust heated by ultraviolet radiation from the star, emit strongly at infrared wavelengths (IR) and often appear as arc-shaped or bubble-like features, with the leading edge being more pronounced in the direction of the star's motion. They are also potential sites for particle acceleration, where particles may reach relativistic speeds and emit radiation across the electromagnetic spectrum. This possibility has been explored in previous studies, such as in Benaglia et al. (2010), who detected the first non-thermal radio bow shock. Recent advancements, particularly the improvement of sensitivity in existing radio interferometers in the northern hemisphere and the addition of very sensitive ones in the southern hemisphere, have led to multiple radio detections of bow shocks and have allowed for spectral index studies (van den Eijnden et al., 2022; Van den Eijnden et al., 2022; Moutzouri et al., 2022).

In this work we review in Sect. 2 the discovery of new massive O and Be runaway stars

Table 1: Main characteristics of works on all-sky searches of runaways among O, B, Be and young stars in the Milky Way, except for two references of the LMC and SMC.

Sample	Method	Threshold	Runaways	References
O stars	3D vel.	$30\,\mathrm{km\,s^{-1}}$	$\sim 20\%$	Bla61
O stars	3D vel.	$40\,\mathrm{km\,s^{-1}}$	$\sim 49\%$	Sto79
≤ 50 Myr & *Hipparcos*	3D vel.	$28\,\mathrm{km\,s^{-1}}$	$\sim 27\%$	Tet11
O stars & *Gaia* DR1	2D p.m.	None	$\sim 6\%$	MAp18
O stars in 30 Dor (LMC)	1D vel.	None	$\sim 7\%$	San22
GOSC & *Gaia* EDR3	2D vel.	$25\,\mathrm{km\,s^{-1}}$	$\sim 22\%$	Kob22
GOSC-*Gaia* DR3	2D vel.	None	25.4%	CCa23
OB stars in SMC	1D vel.	$30\,\mathrm{km\,s^{-1}}$	11%	Lam16
B stars	3D vel.	$30\,\mathrm{km\,s^{-1}}$	$\sim 2\%$	Bla61
Be & *Gaia* DR1	3D vel.	None	$\sim 13\%$	Bou18
BeSS-*Gaia* DR3	2D vel.	None	5.2%	CCa23

Reference: Bla61 – Blaauw (1961); Sto79 – Stone (1979); Tet11 – Tetzlaff et al. (2011); MAp18 – Maíz Apellániz et al. (2018); San22 – Sana et al. (2022); Kob22 – Kobulnicky and Chick (2022); CCa23 – Carretero-Castrillo et al. (2023a); Lam16 – Lamb et al. (2016); Bou18 – Boubert and Evans (2018)

with *Gaia* DR3 already published in Carretero-Castrillo et al. (2023a), some of which may represent high-mass X-ray or gamma-ray binaries (Ayan-Míguez and Ribó, 2019; Carretero-Castrillo et al., 2023b). In addition, we also searched for stellar bow shocks around these runaways (Carretero-Castrillo+24, submitted to A&A), and present a summary of this work in Sect. 3. We comment on future prospects to find new binary systems and high-energy sources within our samples in Sect. 4. Finally, we state our conclusions in Sect. 5.

2. Search for Runaway Stars with *Gaia* DR3

2.1. Data

Gaia, a mission by the European Space Agency (ESA) launched in December 2013, is mapping the three-dimensional spatial and velocity distribution of over a billion stars and determining their astrophysical properties (*Gaia* Collaboration: Prusti et al., 2016). Throughout the mission, several *Gaia* data releases have progressively improved in astrometry and provided increasing amounts of information (positions, proper motions, parallaxes, temperatures, radial velocities, etc.). For this study, we utilize data from the DR3 release (*Gaia* Collaboration: Vallenari et al., 2023). Specifically, we focus on the stars belonging to two catalogs of massive stars: the Galactic O-Star Catalog (GOSC) (Maíz Apellániz et al., 2013), which compiles O-type stars in the Milky Way, and the Be Star Spectra (BeSS) catalog (Neiner et al., 2011), containing classical Be stars, Herbig Ae/Be stars, and B[e] supergiants. These catalogs are relevant to search for stellar companions of gamma-ray binaries, which are predominantly O- and Be-type stars.

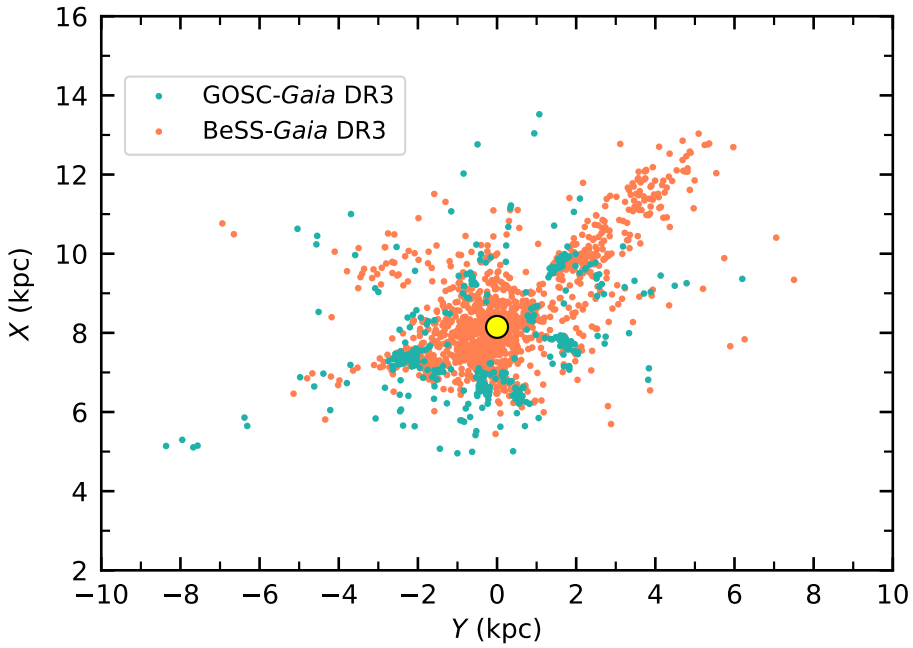

Figure 3: Galactocentric (X,Y) distributions of the GOSC-*Gaia* DR3 stars (light green), and the BeSS-*Gaia* DR3 stars (orange). The position of the Sun is marked with a yellow circle at $(X,Y) = (8.15,0)$ kpc. Adapted from Carretero-Castrillo et al. (2023a, Fig. 3) – CC BY 4.0.

We use a version of GOSC containing 643 O and BA stars, but remove two A0stars and 37 stars flagged as multiple star systems to avoid astrometric problems with *Gaia* data, ending with 604 stars. We cross-match their positions with *Gaia*-DR3 ones allowing for a maximum separation of $0.5''$, yielding 600 cross matches. However, some of these matches are due to two different *Gaia* sources coincident with a single GOSC star. We remove these cases and loose six stars, ending up with 598 stars. Afterwards we apply different quality cuts to the resulting catalog to ensure a good quality of the astrometric data and remove: stars in pairs with the same *Gaia* `source_id`, stars with non 5- or 6-parameter solution, stars with magnitude $G < 6$, stars with `visibility_periods_used` < 10, stars with a parallax error over parallax greater than 0.2, stars with negative parallaxes, and stars with a RUWE parameter greater than 1.35. We also reject six stars with galactocentric distances smaller than 5 kpc because of the validity range of the Galactic rotation curve used. This yields a subset of 417 stars stars, which we call the GOSC-*Gaia* DR3 catalog. For the BeSS catalog, containing 2330 Be stars, we conduct a similar process and remove Herbig Ae/Be stars and B[e] supergiants, stars in the LMC or SMC, we use a maximum separation for the cross match of $1.5''$ due to the limited astrometric quality in the BeSS database, and we apply the same quality cuts mentioned above. We end up with a refined catalog of 1335 stars that we call the BeSS-*Gaia* DR3 catalog.

Gaia DR3 provides very accurate positions, proper motions and parallaxes of the stars under study. To derive their distances and related uncertainties we use the procedure described in Maíz Apellániz (2022). The Galactocentric (X,Y) distributions of the stars in the GOSC- and BeSS-*Gaia* DR3 catalogs are presented in Fig. 3. We note that the overdensity

Table 2: Means and standard deviations of the velocity distributions for the field stars. Adapted from Carretero-Castrillo et al. (2023a).

Catalog	Stars	Field Stars	$\mu^{\rm GF}_{\rm V_{TAN}} \pm \sigma^{\rm GF}_{\rm V_{TAN}}$	$\mu^{\rm GF}_{\rm W_{RSR}} \pm \sigma^{\rm GF}_{\rm W_{RSR}}$
	#	#	(km s^{-1})	(km s^{-1})
GOSC-*Gaia* DR3	417	311	1.0 ± 6.6	-1.0 ± 5.3
BeSS-*Gaia* DR3	1335	1266	1.6 ± 9.3	-0.5 ± 4.9

of BeSS-*Gaia* DR3 stars in the direction from the Sun toward $(X,Y) = (13,5)$ kpc is due to low-resolution surveys of Be stars in that particular direction.

2.2. Method

To detect runaway stars, we first need to compute their velocities. To this end we need positions, parallaxes, proper motions and radial velocities. However, *Gaia* DR3 does not provide many radial velocities for O and Be stars. Therefore, we assume a Galactic rotation curve (model A5 of Reid et al., 2019) from which we compute a theoretical radial velocity (i.e., the radial velocity the star would have if it was moving following the Galactic rotation curve). We then apply the usual reference system transformations from the Local Standard of Rest (LSR) to the Regional Standard of Rest (RSR) from Johnson and Soderblom (1987). Finally, we define a new reference system, composed of the tangential velocity $V_{\rm TAN}$, which is contained in the plane of the sky and is parallel to the Galactic plane, the line of sight velocity $V_{\rm LOS}$, and the velocity component $W_{\rm RSR}$ that is perpendicular to this plane. The different reference systems are shown in Fig. 4. We finally use the 2D velocity system composed of $V_{\rm TAN}$ and $W_{\rm RSR}$. For further details about the methodology and related propagation of uncertainties we refer the reader to Carretero-Castrillo et al. (2023a).

Second, we need to define a runaway criterion. We classified the runaway stars based on how significant the 2D velocities of the stars are with respect to the mean Galactic rotation. To do this, we used the E parameter presented in Eq. (1), which takes into account the means and standard deviations of Gaussian fits to the velocity distributions of the field stars ($\mu^{\rm GF}_{V_{\rm TAN}}, \mu^{\rm GF}_{W_{\rm RSR}}, \sigma^{\rm GF}_{V_{\rm TAN}}, \sigma^{\rm GF}_{W_{\rm RSR}}$), the individual errors of the stars ($\sigma_{V_{\rm TAN,*}}, \sigma_{W_{\rm RSR,*}}$), and is normalized to a 3-sigma–confidence level. Therefore, after applying an iterative 3-σ clipping process, stars with $E > 1$ are classified as runaway stars, while stars with $E < 1$ are classified as field stars.

$$E = \sqrt{\left(\frac{V_{\rm TAN} - \mu^{\rm GF}_{V_{\rm TAN}}}{3\sqrt{{\sigma^{\rm GF}_{V_{\rm TAN}}}^2 + \sigma^2_{V_{\rm TAN,*}}}}\right)^2 + \left(\frac{W_{\rm RSR} - \mu^{\rm GF}_{W_{\rm RSR}}}{3\sqrt{{\sigma^{\rm GF}_{W_{\rm RSR}}}^2 + \sigma^2_{W_{\rm RSR,*}}}}\right)^2}. \quad (1)$$

2.3. Results and discussion

The means and standard deviations obtained from the final Gaussian fits to the velocity distributions of the field stars, which are used in Eq. 1, are presented in Table 2. Notably, $\sigma^{\rm GF}_{V_{\rm TAN}}$ is greater than $\sigma^{\rm GF}_{W_{\rm RSR}}$ for both catalogs, with BeSS-*Gaia* DR3 stars exhibiting a higher $\sigma^{\rm GF}_{V_{\rm TAN}}$ than

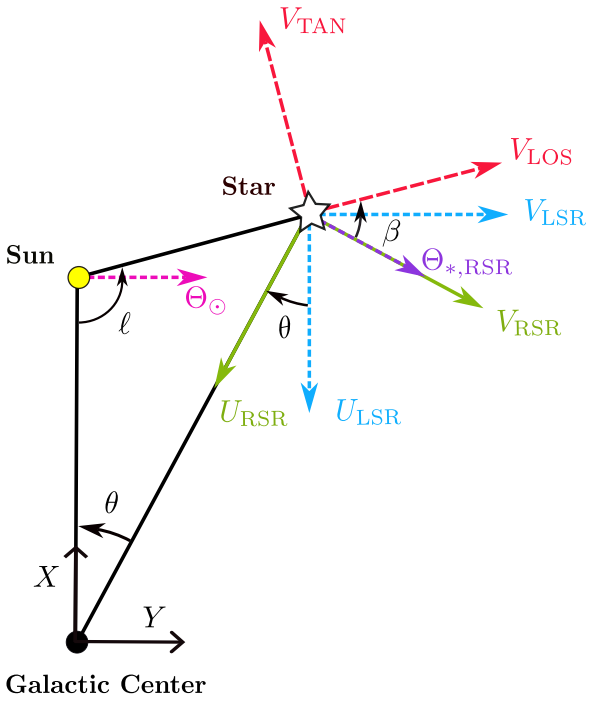

Figure 4: Reference systems used in this work, depicted in the Galactic XY plane. The Sun and the Galactic Center (GC) are indicated with a yellow and black circle, respectively. The white star represents a given star in our catalogs. ℓ is the Galactic longitude, θ is the angle between the star and the Sun as seen from the GC and β is a rotation angle that we use to shift from RSR to the new reference system. The Galactic circular rotation velocity is $\Theta_\odot$ at the position of the Sun and $\Theta_{*,\rm RSR}$ at the position of the star. LSR and RSR velocities are shown in light blue and green, respectively. The tangential velocity $V_{\rm TAN}$ and the line-of-sight velocity $V_{\rm LOS}$ are shown in red. The third velocity components of the LSR and the RSR systems, $W_{\rm LSR}$ and $W_{\rm RSR}$, are not shown in the figure because they are perpendicular to this plane. Adapted from Carretero-Castrillo et al. (2023a, Fig. 4) – CC BY 4.0.

Table 3: Means and standard deviations of the velocity distributions for the runaway stars. Excerpt from Carretero-Castrillo et al. (2023a, Table 2) – CC BY 4.0.

Catalog	Stars	Runaway Stars	$\mu_{V_{TAN}} \pm \sigma_{V_{TAN}}$	$\mu_{W_{RSR}} \pm \sigma_{W_{RSR}}$
	#	#	(km s^{-1})	(km s^{-1})
GOSC-*Gaia* DR3	417	106	-3.1 ± 39.7	1.1 ± 38.7
BeSS-*Gaia* DR3	1335	69	-7.7 ± 34.6	1.0 ± 22.3

those from GOSC-*Gaia* DR3 because they are more affected by Galactic velocity diffusion in the disk (see Carretero-Castrillo et al. 2023a for additional checks to reach this conclusion).

After applying the methodology described in the previous subsection, we identified 106 runaway stars in the GOSC-*Gaia* DR3 catalog (42 newly discovered) and 69 in the BeSS-*Gaia* DR3 catalog (47 newly discovered), representing 25.4% and 5.2% of the catalogs, respectively. The means and standard deviations (without applying Gaussian fits) to the velocity distribution of the runaway stars are presented in Table 3.

Runaway stars exhibit high velocity dispersions of 20–40 km s^{-1}, consistent with literature values (Stone, 1991; Tetzlaff et al., 2011). Figures 5 and 6 show the 2D (V_{TAN}, W_{RSR}) velocity distributions for the GOSC- and BeSS-*Gaia* DR3 catalogs, respectively, including a color distinction between runaways and field stars. Field stars are clustered around $(0,0)$ while runaway stars present higher velocities. In particular, the velocities of the O runaway stars are higher than those of Be runaways. The lower standard deviations in W_{RSR} together with the larger uncertainties in V_{TAN} imply that more runaways are identified in the W_{RSR} component.

The positions in Galactic coordinates of both the O and Be runaway stars are shown as yellow circles in Fig. 7, together with their positions up to 3 Myr in the future indicated with orange traces. The runaway stars present two to three times more dispersion in galactic latitude than the field stars (not shown here), which is expected given that they have been expelled from their birthplaces during their formation as runaways.

We also classified the runaways in different sub-spectral type bins and found that the runaway percentage decreases as we move to later spectral types. Table 4 shows the results in number and percentage. The higher percentages and higher velocities found for O-type stars compared to Be-type stars are in favor of the dominance of the DES over the BSS scenario.

3. Search for Stellar Bow Shocks

We conducted a search for stellar bow shocks around the runaways found in Carretero-Castrillo et al. (2023a) using data from the Wide-field Infrared Survey Explorer (WISE) (Wright et al., 2010), which is a NASA-funded mission designed to survey the entire sky in the mid-infrared. Completed in 2010, WISE provided significantly higher sensitivity than previous infrared surveys, mapping the sky in multiple bands with varying resolutions.

Bow shocks are associated with warm dust emission, and this emission is primarily expected in the WISE $W4$ band (22 µm). Therefore, we utilized the $W4$ band to search for bow

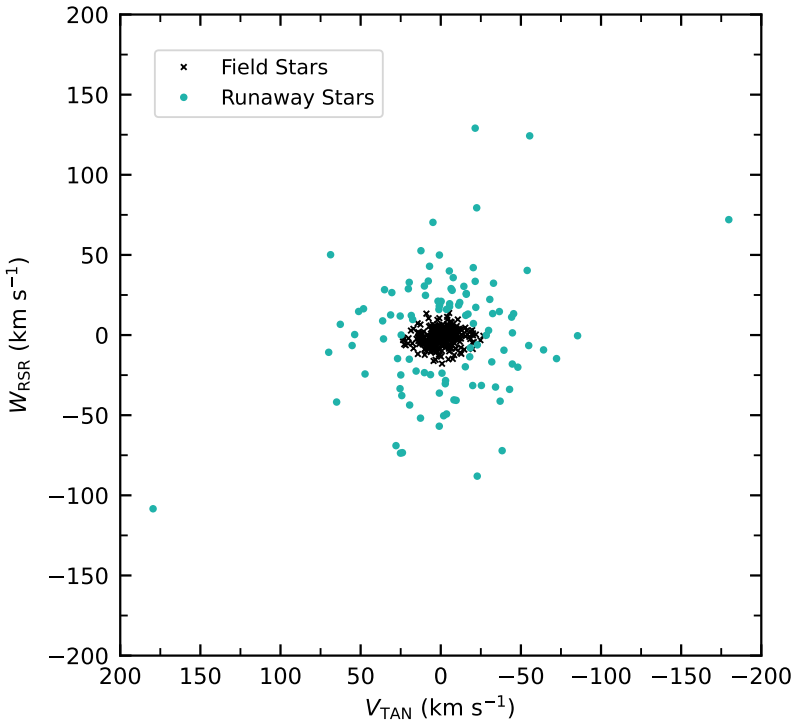

Figure 5: W_{RSR} as a function of V_{TAN} for the GOSC-*Gaia* DR3 stars. Field stars are depicted in black, and runaway stars are shown in light green. Adapted from Carretero-Castrillo et al. (2023a, Fig. 8) – CC BY 4.0.

Table 4: Field and runaway stars as a function of spectral type. Adapted from Carretero-Castrillo et al. (2023a, Table 5) – CC BY 4.0.

Spectral Type	**Stars**	**Runaway Stars**	
	#	**#**	**%**
O2–O7	199	50	25.1
O8–O9	194	46	23.7
B0e–B3e	585	36	6.2
B4e–B9e	482	23	4.8

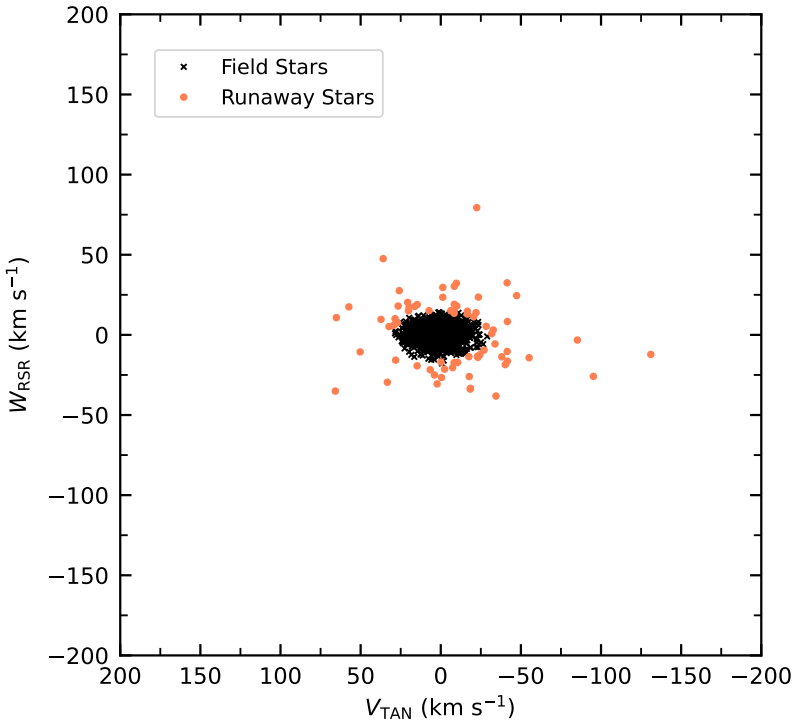

Figure 6: W_{RSR} as a function of V_{TAN} for the BeSS-*Gaia* DR3 stars. Field stars are depicted in black, and runaway stars are shown in orange. Adapted from Carretero-Castrillo et al. (2023a, Fig. 9) – CC BY 4.0.

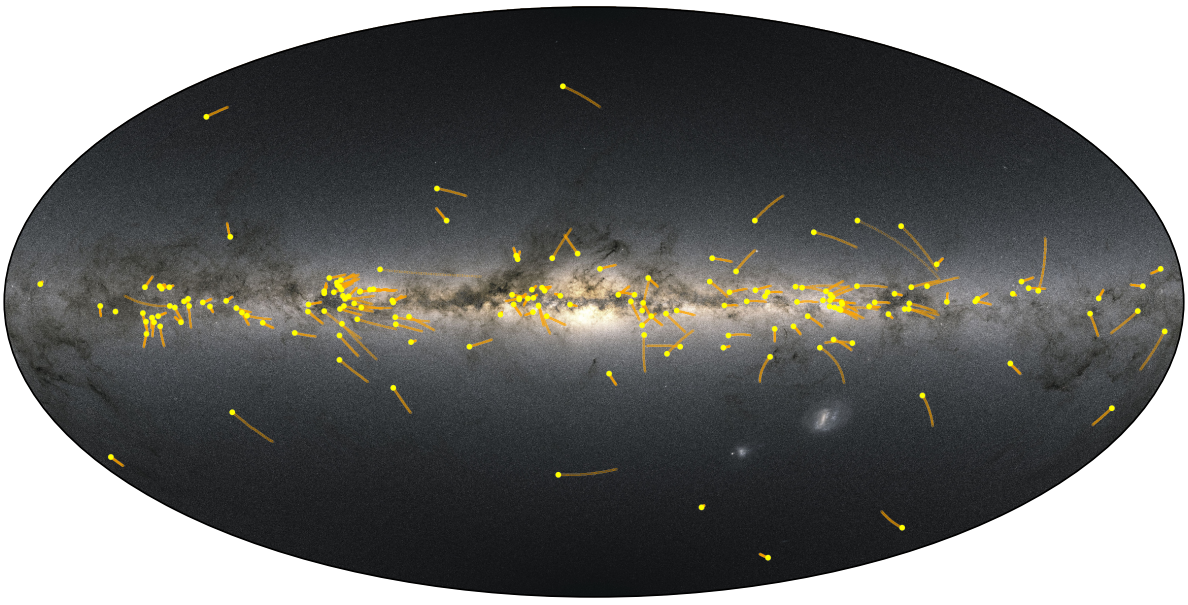

Figure 7: All-sky view in Galactic coordinates showing the O and Be runaway stars found in the GOSC- and BeSS-*Gaia* DR3 catalogs as yellow circles. Orange traces indicate the positions of the stars up to 3 Myr in the future. The background sky map of the Milky Way is that of *Gaia* DR3 (Credits: ESA/*Gaia*/DPAC – CC BY-SA 3.0 IGO).

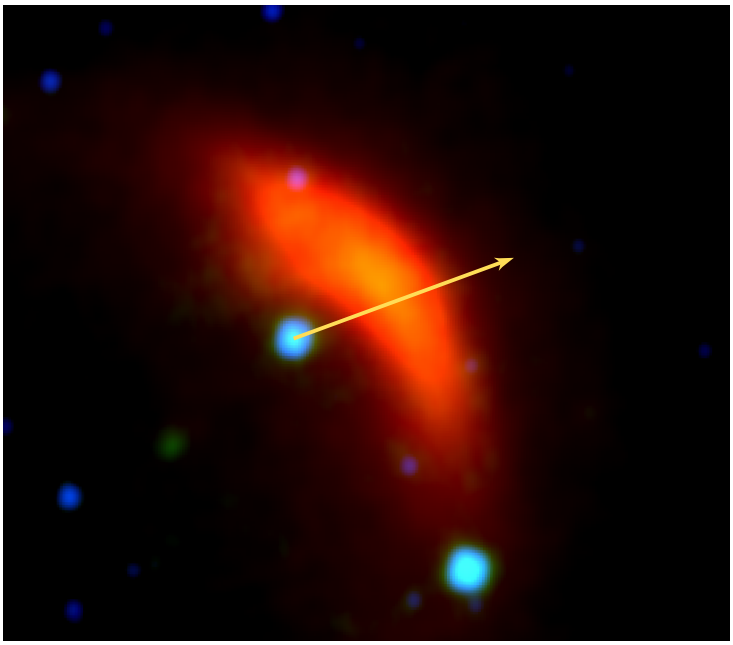

Figure 8: WISE image of a known bow shock as an example.

shock or bubble-like structures around runaway stars. In addition, we corrected the *Gaia* DR3 proper motions to account for the ISM motion caused by Galactic rotation. For this, we used the prescription provided in Comerón and Pasquali (2007). In this way, we can know the actual motion of the runaway stars with respect to the bow shock candidate. Therefore, we classified an IR structure as a stellar bow shock or bubble if it was close to the position of the star and showed an arc-shaped structure/or the rim of the bubble in the direction of the runaway star's corrected proper motion.

We found 13 new stellar bow shock or bubble candidates, mostly associated with O-type stars. We also identified 16 known bow shocks or bubble candidates discovered in previous works. Figure 8 presents an example of a WISE RGB image in $W4+W3+W2$ of one of these known bow shocks. Additionally, we introduced a new category of "mini-bubble" sources which are around twice the W4 PSF, with two examples linked to Be-type stars. We performed an IR geometrical characterization of the bow shocks and bubbles, measuring projected distances such as the stand-off distance R, the length, and the width. Using these measurements, we estimated the ISM densities at the bow shock positions using the following equation, adapted from Wilkin (1996):

$$R_0 = \sqrt{\frac{\dot{M} v_\infty}{4\pi \mu n_{\rm ISM} {V_{\rm PEC}^{\rm 3D}}^2}} \tag{2}$$

where R_0 is the stand-off distance, $\dot{M}$ is the mass-loss rate, v_∞ is the wind terminal velocity, μ is the mass of the ISM per H atom, and $V_{\rm PEC}^{\rm 3D}$ is the three dimensional (3D) peculiar velocity of the star. Using the projected stand-off distance R instead of R_0, we found a median $n_{\rm ISM}$ of $\sim 4\,{\rm cm}^{-3}$. This estimate aligns with previous works, though in some particular cases we obtain very-high density values that may be overestimated due to projection effects.

We also searched for radio emission from the bow shocks using data from surveys like

NVSS, VLASS, and RACS. While we found radio emission coincident with the bow shock position for some sources, the radio morphology differed from the one of the IR bow shock, making it difficult to confirm radio counterparts. We explored both thermal and non-thermal mechanisms as potential origins of the radio emission and predicted the radio flux density for undetected bow shocks as done in Van den Eijnden et al. (2022). Despite the non-detection of the sources, they remain consistent with the possibility to display non-thermal radio emission that could be detected in deeper surveys.

Overall, our results highlight the need for more sensitive radio observations to confirm bow shocks at radio wavelengths and investigate the physical processes driving their radio and high-energy emissions. Instruments like the Very Large Array (VLA) could play a crucial role in uncovering a new population of radio bow shocks. As work in progress, we are now analyzing VLA data of eight bow shock candidates found in this work.

4. Search for Binaries

As mentioned in the introduction, the BSS can result in systems such as HMXBs and gamma-ray binaries. We looked for known of these sources among our runaways and found six HMXBs and one gamma-ray binary. In particular, we identified the gamma-ray binary LS 5039 and the HMXBs Vela X-1, 4U 1700−377, IGR J08408−4503, and Cygnus X–1 in the GOSC-*Gaia* DR3 catalog. From the BeSS-*Gaia* DR3 runaways, we found the SAX J2103.5+4545 and V 0332+53 HMXBs. Notably, Vela X-1 and SAX J2103.5+4545 are identified here as runaway HMXBs for the first time.

As an outlook, on the one hand, we want to search for binarity hints among our runaways to create a reduced list of runaway binary systems candidates. To this end, we will check for radial velocity variations and signatures of fast rotation (Britavskiy et al., 2023; Holgado et al., 2022). On the other hand, since HMXBs and gamma-ray binaries present emission in different wavelengths, we are conducting a multi-wavelength study (from radio to high-energy gamma rays) of this sample to create a reduced list of high-energy binary candidates. Once we have a reduced list of interesting objects, we plan to prepare observations of the most promising candidates to be HMXBs and gamma-ray binaries. This could potentially help to answer open questions for gamma-ray binaries, of which we only know nine systems at the time of writing.

5. Conclusions

In this work we have summarized the status of our ongoing project to find new runaway stars, study their interaction with the ISM and search for high-energy binary systems. In particular, we reach the following conclusions for each topic:

- **Runaway stars.** After using *Gaia* DR3 data and the GOSC and BeSS catalogs we have detected 175 runaways, 89 of which are new discoveries. We have found that $\sim 25\%$ of O-type stars from our sample are runaways, while for Be-type stars this decreases to $\sim 5\%$. O-type stars runaways have higher velocities than B-type ones. These results

suggest that the dynamical ejection scenario is more likely than the supernova explosion scenario.

- **Bow shocks.** We have used WISE infrared images to discover 13 new stellar bow shocks and bubbles around the runaway stars. We have characterized their morphology and derived ISM densities. The analysis of VLA observations of some of these sources is ongoing.

- **High-energy binary systems.** Among the sample of runaways stars we have found one gamma-ray binary and six HMXBs. Ongoing multi-wavelength studies to search for binarity and high-energy emission could provide the discovery of new such systems.

Acknowledgments

We would like to thank the members of the *Gaia* team at Universitat de Barcelona for many useful discussions. We thank J. Maíz Apellániz, S. R. Berlanas, S. Simón-Díaz, C. Martínez-Sebastián, M. Pantaleoni González, G. Holgado and A. de Burgos for valuable insights and feedback. We acknowledge financial support from the State Agency for Research of the Spanish Ministry of Science and Innovation under grants PID2022-136828NB-C41/AEI/10.13039/501100011033/ERDF/EU and PID2022-138172NB-C43/AEI/10.13039/501100011033/ERDF/EU, and through the Unit of Excellence María de Maeztu 2020–2023 award to the Institute of Cosmos Sciences (CEX2019-000918-M). We acknowledge financial support from Departament de Recerca i Universitats of Generalitat de Catalunya through grant 2021SGR00679. MC-C acknowledges the grant PRE2020-094140 funded by MCIN/AEI/10.13039/501100011033 and FSE/ESF funds. Figure 7 was generated using the `mw-plot` Python package. This work has made use of data from the European Space Agency (ESA) mission *Gaia* (https://www.cosmos.esa.int/gaia), processed by the *Gaia* Data Processing and Analysis Consortium (DPAC, https://www.cosmos.esa.int/web/gaia/dpac/consortium). Funding for the DPAC has been provided by national institutions, in particular the institutions participating in the *Gaia* Multilateral Agreement. This work has made use of the BeSS database, operated at LESIA, Observatoire de Meudon, France http://basebe.obspm.fr. This publication makes use of data products from the Wide-field Infrared Survey Explorer, which is a joint project of the University of California, Los Angeles, and the Jet Propulsion Laboratory/California Institute of Technology, funded by the National Aeronautics and Space Administration. This research has made use of NASA's Astrophysics Data System. This research has made use of the SIMBAD database, operated at CDS, Strasbourg, France.

Further Information

Authors' ORCID identifiers

0000-0002-1426-1311 (Mar CARRETERO-CASTRILLO)
0000-0001-6944-6383 (Marc RIBÓ)

0000-0002-1566-9044 (Josep M. PAREDES)
0000-0002-6683-3721 (Paula BENAGLIA)

Author contributions

MC-C: data curation, formal analysis, investigation, methodology, project administration, software, visualization, writing-original draft;

MR: conceptualization, funding acquisition, investigation, methodology, supervision, writing-original draft;

JMP: conceptualization, funding acquisition, investigation, supervision;

PB: conceptualization, data curation, formal analysis, investigation.

Conflicts of interest

The authors declare no conflict of interest.

References

Ayan-Míguez, I. and Ribó, M. (2019) Searching for gamma-ray binaries using GOSC and Gaia DR2. In *High Energy Phenomena in Relativistic Outflows VII (HEPRO VII)*, *Proceedings of Science*, volume 354. Sissa Medialab. https://doi.org/10.22323/1.354.0095.

Benaglia, P., Romero, G. E., Martí, J., Peri, C. S., and Araudo, A. T. (2010) Detection of nonthermal emission from the bow shock of a massive runaway star. *A&A*, **517**, L10. https://doi.org/10.1051/0004-6361/201015232.

Blaauw, A. (1961) On the origin of the O- and B-type stars with high velocities (the "run-away" stars), and some related problems. *BAN*, **15**, 265–290. https://ui.adsabs.harvard.edu/abs/1961BAN....15..265B.

Boubert, D. and Evans, N. W. (2018) On the kinematics of a runaway Be star population. *MNRAS*, **477**(4), 5261–5278. https://doi.org/10.1093/mnras/sty980.

Britavskiy, N., Simón-Díaz, S., Holgado, G., Burssens, S., Maíz Apellániz, J., Eldridge, J. J., Nazé, Y., Pantaleoni González, M., and Herrero, A. (2023) The IACOB project. VIII. Searching for empirical signatures of binarity in fast-rotating O-type stars. *A&A*, **672**, A22. https://doi.org/10.1051/0004-6361/202245145.

Carretero-Castrillo, M., Ribó, M., and Paredes, J. M. (2023a) Galactic runaway O and Be stars found using *Gaia* DR3. *A&A*, **679**, A109. https://doi.org/10.1051/0004-6361/202346613.

Carretero-Castrillo, M., Ribó, M., and Paredes, J. M. (2023b) Search for new gamma-ray binaries among runaway stars. In *7th Heidelberg International Symposium on High-Energy Gamma-Ray Astronomy (Gamma2022)*, *Proceedings of Science*, volume 417. Sissa Medialab, Trieste (IT). https://doi.org/10.22323/1.417.0133.

Chini, R., Hoffmeister, V. H., Nasseri, A., Stahl, O., and Zinnecker, H. (2012) A spectroscopic survey on the multiplicity of high-mass stars: Multiplicity of high-mass stars. *MNRAS*, **424**(3), 1925–1929. https://doi.org/10.1111/j.1365-2966.2012.21317.x.

Comerón, F. and Pasquali, A. (2007) A very massive runaway star from Cygnus OB2. *A&A*, **467**(1), L23–L27. https://doi.org/10.1051/0004-6361:20077304.

Dorigo Jones, J., Oey, M. S., Paggeot, K., Castro, N., and Moe, M. (2020) Runaway OB stars in the Small Magellanic Cloud: Dynamical versus supernova ejections. *ApJ*, **903**(1), 43. https://doi.org/10.3847/1538-4357/abbc6b.

Dubus, G. (2013) Gamma-ray binaries and related systems. *A&ARv*, **21**, 64. https://doi.org/10.1007/s00159-013-0064-5.

Gaia Collaboration: Prusti, T., de Bruijne, J. H. J., Brown, A. G. A., Vallenari, A., Babusiaux, C., Bailer-Jones, C. A. L., Bastian, U., Biermann, M., Evans, D. W., Eyer, L., and *615 more* (2016) The *Gaia* mission. *A&A*, **595**, A1. https://doi.org/10.1051/0004-6361/201629272.

Gaia Collaboration: Vallenari, A., Brown, A. G. A., Prusti, T., de Bruijne, J. H. J., Arenou, F., Babusiaux, C., Biermann, M., Creevey, O. L., Ducourant, C., Evans, D. W., and *445 more* (2023) *Gaia* Data Release 3: Summary of the content and survey properties. *A&A*, **674**, A1. https://doi.org/10.1051/0004-6361/202243940.

Holgado, G., Simón-Díaz, S., Herrero, A., and Barbá, R. H. (2022) The IACOB project. VII. The rotational properties of Galactic massive O-type stars revisited. *A&A*, **665**, A150. https://doi.org/10.1051/0004-6361/202243851.

Johnson, D. R. H. and Soderblom, D. R. (1987) Calculating Galactic space velocities and their uncertainties, with an application to the Ursa Major group. *AJ*, **93**, 864–867. https://doi.org/10.1086/114370.

Kobulnicky, H. A. and Chick, W. T. (2022) Kinematics of the central stars powering bowshock nebulae and the large multiplicity fraction of runaway OB stars. *AJ*, **164**(3), 86. https://doi.org/10.3847/1538-3881/ac7f2b.

Lamb, J. B., Oey, M. S., Segura-Cox, D. M., Graus, A. S., Kiminki, D. C., Golden-Marx, J. B., and Parker, J. W. (2016) The Runaways and Isolated O-type Star Spectroscopic Survey of the SMC (RIOTS4). *ApJ*, **817**(2), 113. https://doi.org/10.3847/0004-637X/817/2/113.

Maíz Apellániz, J. (2022) An estimation of the *Gaia* EDR3 parallax bias from stellar clusters and Magellanic Clouds data. *A&A*, **657**, A130. https://doi.org/10.1051/0004-6361/202142365.

Maíz Apellániz, J., Pantaleoni González, M., Barbá, R. H., Simón-Díaz, S., Negueruela, I., Lennon, D. J., Sota, A., and Trigueros Páez, E. (2018) Search for Galactic runaway stars using *Gaia* Data Release 1 and HIPPARCOS proper motions. *A&A*, **616**, A149. https://doi.org/10.1051/0004-6361/201832787.

Maíz Apellániz, J., Sota, A., Morrell, N. I., Barbá, R. H., Walborn, N. R., Alfaro, E. J., Gamen, R. C., Arias, J. I., and Gallego Calvente, A. T. (2013) The Galactic O-star Spectroscopic Catalog (GOSC) and Survey (GOSSS): first whole-sky results and further updates. In *Massive Stars: From α to Ω*. https://ui.adsabs.harvard.edu/abs/2013msao.confE.198M.

Marchant, P. and Bodensteiner, J. (2024) The evolution of massive binary stars. *ARA&A*, **62**, 21–61. https://doi.org/10.1146/annurev-astro-052722-105936.

Moutzouri, M., Mackey, J., Carrasco-González, C., Gong, Y., Brose, R., Zargaryan, D., Toalá, J. A., Menten, K. M., Gvaramadze, V. V., and Rugel, M. R. (2022) And then they were two: Detection of non-thermal radio emission from the bow shocks of two runaway stars. *A&A*, **663**, A80. https://doi.org/10.1051/0004-6361/202243098.

Neiner, C., de Batz, B., Cochard, F., Floquet, M., Mekkas, A., and Desnoux, V. (2011) The Be Star Spectra (BeSS) database. *AJ*, **142**(5), 149. https://doi.org/10.1088/0004-6256/142/5/149.

Pflamm-Altenburg, J. and Kroupa, P. (2010) The two-step ejection of massive stars and the issue of their formation in isolation. *MNRAS*. https://doi.org/10.1111/j.1365-2966.2010.16376.x.

Poveda, A., Ruiz, J., and Allen, C. (1967) Run-away stars as the result of the gravitational collapse of proto-stellar clusters. *BOTT*, **4**(28), 86–90.

Reid, M. J., Menten, K. M., Brunthaler, A., Zheng, X. W., Dame, T. M., Xu, Y., Li, J., Sakai, N., Wu, Y., Immer, K., Zhang, B., Sanna, A., Moscadelli, L., Rygl, K. L. J., Bartkiewicz, A., Hu, B., Quiroga-Nuñez, L. H., and van Langevelde, H. J. (2019) Trigonometric parallaxes of high-mass star-forming regions: Our view of the Milky Way. *ApJ*, **885**(2), 131. https://doi.org/10.3847/1538-4357/ab4a11.

Rivinius, T., Carciofi, A. C., and Martayan, C. (2013) Classical Be stars: Rapidly rotating B stars with viscous Keplerian decretion disks. *A&ARv*, **21**, 69. https://doi.org/10.1007/s00159-013-0069-0.

Sana, H., de Mink, S. E., de Koter, A., Langer, N., Evans, C. J., Gieles, M., Gosset, E., Izzard, R. G., Le Bouquin, J.-B., and Schneider, F. R. N. (2012) Binary interaction dominates the evolution of massive stars. *Sci*, **337**, 444–446. https://doi.org/10.1126/science.1223344.

Sana, H., Ramírez-Agudelo, O. H., Hénault-Brunet, V., Mahy, L., Almeida, L. A., de Koter, A., Bestenlehner, J. M., Evans, C. J., Langer, N., Schneider, F. R. N., Crowther, P. A., de Mink, S. E., Herrero, A., Lennon, D. J., Gieles, M., Maíz Apellániz, J., Renzo, M., Sabbi, E., van Loon, J. T., and Vink, J. S. (2022) The VLT-FLAMES Tarantula Survey: Observational evidence for two distinct populations of massive runaway stars in 30 Doradus. *A&A*, **668**, L5. https://doi.org/10.1051/0004-6361/202244677.

Slettebak, A. (1988) The Be stars. *PASP*, **100**, 770–784. https://doi.org/10.1086/132234.

Stone, R. C. (1979) Kinematics, close binary evolution, and ages of the O stars. *ApJ*, **232**, 520–530. https://doi.org/10.1086/157311.

Stone, R. C. (1991) The space frequency and origin of the runaway O and B stars. *AJ*, **102**, 333–349. https://doi.org/10.1086/115880.

Tetzlaff, N., Neuhäuser, R., and Hohle, M. M. (2011) A catalogue of young runaway *Hipparcos* stars within 3 kpc from the Sun. *MNRAS*, **410**(1), 190–200. https://doi.org/10.1111/j.1365-2966.2010.17434.x.

van den Eijnden, J., Heywood, I., Fender, R., Mohamed, S., Sivakoff, G. R., Saikia, P., Russell, T. D., Motta, S., Miller-Jones, J. C. A., and Woudt, P. A. (2022) MeerKAT discovery of radio emission from the Vela X-1 bow shock. *MNRAS*, **510**(1), 515–530. https://doi.org/10.1093/mnras/stab3395.

Van den Eijnden, J., Saikia, P., and Mohamed, S. (2022) Radio detections of IR-selected runaway stellar bow shocks. *MNRAS*, **512**(4), 5374–5389. https://doi.org/10.1093/mnras/stac823.

Vanbeveren, D., De Loore, C., and Van Rensbergen, W. (1998) Massive stars. *A&ARv*, **9**(1-2), 63–152. https://doi.org/10.1007/s001590050015.

Wilkin, F. P. (1996) Exact analytic solutions for stellar wind bow shocks. *ApJ*, **459**(1). https://doi.org/10.1086/309939.

Woosley, S. and Bloom, J. (2006) The supernova–gamma-ray burst connection. *ARA&A*, **44**, 507–556. https://doi.org/10.1146/annurev.astro.43.072103.150558.

Wright, E. L., Eisenhardt, P. R. M., Mainzer, A. K., Ressler, M. E., Cutri, R. M., Jarrett, T., Kirkpatrick, J. D., Padgett, D., McMillan, R. S., Skrutskie, M., Stanford, S. A., Cohen, M., Walker, R. G., Mather, J. C., Leisawitz, D., Gautier, T. N., McLean, I., Benford, D., Lonsdale, C. J., Blain, A., Mendez, B., Irace, W. R., Duval, V., Liu, F., Royer, D., Heinrichsen, I., Howard, J., Shannon, M., Kendall, M., Walsh, A. L., Larsen, M., Cardon, J. G., Schick, S., Schwalm, M., Abid, M., Fabinsky, B., Naes, L., and Tsai, C.-W. (2010) The Wide-field Infrared Survey Explorer (WISE): Mission description and initial on-orbit performance. *AJ*, **140**(6), 1868–1881. https://doi.org/10.1088/0004-6256/140/6/1868.